On the impact of additive disturbances on Auto-Steering Systems

I. Ballesteros-Tolosana [*,**] **S. Olaru** [*] **P. Rodriguez-Ayerbe** [*] **M. Hovd** [***] **R. Deborne** [**] **G. Pita-Gil** [**]

[*] *Laboratory of Signals and Systems (L2S), Centrale-Supèlec, CNRS, Université de Paris-Saclay, France. (e-mail: name.surname@centralesupelec.fr)*
[**] *Renault SAS, DEA-SAD5 Developtment of ADAS control laws (e-mail: name.surname@renault.com)*
[***] *Department of Engineering Cybernetics, Norwegian University of Science and Technology, Trondheim, Norway (e-mail: name.surname@ntnu.no)*

Abstract: Several control techniques are available for the automotive systems and their design is often based on the available measurements of different parameters and the integration of the hard input and performance constraints. The objective of the present study is to revisit the closed loop dynamics of an auto-steering system to offer an evaluation of the impact of the curvature of the road. From a theoretical point of view, robust positive invariance theory is presented in order to perform the analysis of the effects that a bounded parameter-varying additive disturbance has on a linear parameter-varying controller used to ensure stability of a model predictive control strategy.

Keywords: Automotive control, Predictive control, LPV control, Bounded additive disturbances, Robust Positive Invariance.

1. INTRODUCTION

The automotive industry is increasingly pushing towards the *autonomous driving* concept, considered the future of this business. In this kind of driving, the human plays the role of a passive passenger while the vehicle is completely in charge of the driving task. It can be seen nowadays that several companies are developing prototypes that are capable of autonomously driving the vehicle without human intervention. Nevertheless, there is a long way to go between the *proof-of-concept* and the actual spreading of the technology to the general public.

There are several reasons that can justify this time gap, like the current price of the technology, which is not affordable for most of the vehicle consumers. Then, the drivers learning curve in view of a responsible use and acceptation of such technologies. A natural evolution process is needed at the vehicle industry, where car manufacturers consider that the development of the Advanced Driving Assistance Systems (ADAS) will allow the technology to become mature and progressively lead to Autonomous Driving vehicles. The term ADAS covers the technological systems that, briefly speaking, aim to assist the driver or take over control of the driving task in certain situations, like parking lots, highways or protected roads, offering an improved safety and comfort experience. Nevertheless, as driving conditions are never the same, it becomes a critical feature to come up with robust control strategies that will always keep a correct performance and at the same time ensure system security by constraints handling (Sename et al., 2013), (Ni et al., 2016).

$\star$ The work leading to these results has received funding from the People Programme (Marie Curie Actions) of the European Unions Seventh Framework Programme (FP7/2007-2013) under REA grant agreement no 607957 (TEMPO).

In the present paper, one type of Auto-steering system is studied, the Lane Centering Assistance (LCA) System, which is introduced together with the dynamical model in Section 2. After that, the design of a pre-stabilizing parameter-varying linear controller when the speed of the vehicle changes is presented together with a Model Predictive Control (MPC) strategy to enhance the constraint handling capacities. Thereafter, the objective is to analyze the effect that the curvature of the road, modeled as an additive disturbance that depends on the speed of the vehicle, has on the designed controller and how this uncertainty decreases the domain of attraction of the Linear Parameter Varying (LPV) control and the size of the terminal set for the MPC. In order to perform this analysis, Section 3 introduces the Robust Positive Invariance (RPI) theory tools and different strategies that can be considered when modeling the parameter-varying disturbance. Then, the obtained RPI sets are analyzed and a redesign phase is finally presented in Section 4 together with a simulation example.

2. PRELIMINARIES AND PROBLEM FORMULATION

2.1 Auto-steering System model

The LCA system's main purpose is to stabilize the lateral dynamics of the vehicle to follow the center line of the lane by acting on the steering wheel of the vehicle. When modeling the lateral dynamics of a vehicle, it is common in the literature to adopt the well known *bicycle model* (Rajamani, 2006), as it exhibits a good trade-off between complexity and performance. In the present paper, small slip angles are contemplated, so that the lateral forces are working on their linear region (Pacejka, 2005). Moreover, the interaction between the longitudinal and the lateral forces is not considered, assuming a decoupled

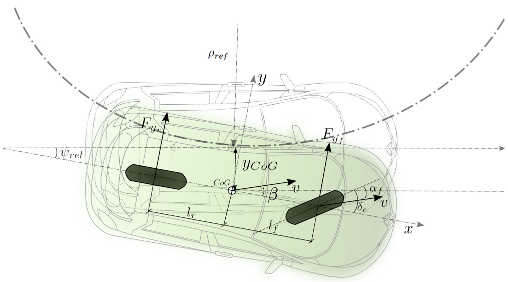

Fig. 1. Bicycle model referenced to the center line

architecture both in the modeling and the control. Finally, the tracking objective of the designed controller will be to stabilize the described lateral dynamics with respect to the center of the road. In this way, the following change of coordinates has been considered, $\dot{\psi}_{rel} = \dot{\psi} - \dot{\psi}_{road} = \dot{\psi} - v_x\rho$, $\dot{y}_{CoG} = \dot{y} - v_x\psi_{rel}$. The resulting dynamical model is depicted in the following:

$$\begin{aligned} \dot{x}(t) &= A(v_x(t))x(t) + Bu(t) \\ y(t) &= Cx(t) \end{aligned} \tag{1}$$

$$A(v_x(t)) = \begin{bmatrix} \frac{-(C_f l_f^2 + C_r l_r^2)}{I_z v_x(t)} & \frac{(C_f l_f - C_r l_r)}{I_z} & \frac{-(C_f l_f - C_r l_r)}{I_z v_x(t)} & 0 \\ 1 & 0 & 0 & 0 \\ \frac{(C_r l_r - C_f l_f)}{m v_x(t)} & \frac{(C_f + C_r)}{m} & \frac{-(C_f + C_r)}{m v_x(t)} & 0 \\ 0 & 0 & 1 & 0 \end{bmatrix}$$

$$B = \left[\frac{C_f l_f}{I_z},\ 0,\ \frac{C_f}{m},\ 0 \right]^T \quad C = \begin{bmatrix} 1 & 0 & 0 & 0 \\ 0 & 1 & 0 & 0 \\ 0 & 0 & 0 & 1 \end{bmatrix}. \tag{2}$$

Where $x(t)$ is the state vector $[\dot{\psi}, \psi_{rel}, \dot{y}_{CoG}, y_{CoG}]^T \in \mathbb{R}^n$. u is the control input $\in \mathbb{R}^p$ which represents the steering wheel angle δ_c and $y \in \mathbb{R}^m$ holds by the vector of system outputs, that will be $[\dot{\psi}, \psi_{rel}, y_{CoG}]^T$. Finally, he term depending on the curvature of the road $-v_x\rho$, is considered in the additive disturbances matrix (See Section 3). Complete measurements of the states are considered in the present study.

The matrices $A(v_x(t)) \in \mathbb{R}^{n\times n}$, $B \in \mathbb{R}^{n\times p}$ depend on several vehicle parameters: C_f and C_r denote the cornering stiffness of the front and rear wheels respectively. The distances from the front and rear axis to the center of gravity are l_f and l_r, m stands for the vehicle mass and I_z for the yaw moment of inertia. All these parameters are considered known and fixed, so they do not introduce any uncertainty to the model.

Finally, the inverse of the longitudinal speed, $\gamma = 1/v_x(t)$ appears linearly in the state matrix (2), playing the role of a varying parameter. In practice, it is measured and bounded $v_x(t) \in \mathcal{V}$, which means that its value is known and its limits are defined by the LCA activation range specifications, $[v_{min}, v_{max}]$. In the following, a discrete-time formulation is used. For doing so, the forward Euler discretization method based on a truncated Taylor series expansion with $T_s = 0.01[s]$ has been applied to the system state-space continuous-time representation displayed in (1), (2).

On top of this formulation, we augment the system state vector $\bar{x}_k^T = [x_k^T \ u_{k-1}^T]^T$ in order to include the control input integrator $\Delta u_k = u_k - u_{k-1}$, also known as *velocity form* (Pannocchia and Rawlings, 2001). This reformulation allows to design a controller that avoids sudden changes in the steering wheel angle. Moreover, in order to have a offset-free tracking of the center of the lane, the integral of the error of the corresponding system state $\int y_{CoG}dt$ is included in the formulation. The augmented system matrices are then defined by $\bar{A}(\gamma_k)$, $\bar{B}$ and $\bar{C} = [C, 0]^T$, with Δu_k being the control input.

$$\bar{A}(\gamma_k) = \begin{bmatrix} I^n + A(\gamma_k)T_s & BT_s \\ 0 & 1 \end{bmatrix} \ \bar{B} = \begin{bmatrix} BT_s \\ 1 \end{bmatrix} \tag{3}$$

Parametric uncertainty representation The uncertainty introduced by varying parameter γ can be expressed in several ways (Kothare et al., 1996), (Bemporad and Morari, 1999). In this application, the parameter is measured and available at any k, so it is possible to express the parameter-varying system dynamics within a polytopic uncertainty representation (Bokor and Balas, 2005): this means that any operating system dynamics at a given speed value within the working range $\bar{A}(1/v_k) = \bar{A}(\gamma_k)$, will be expressed as an affine combination of the two extreme system realizations at the speed limits. Therefore, the system dynamics will be described by the parameter varying model

$$\begin{aligned} \bar{x}_{k+1} &= \bar{A}(\gamma_k)\bar{x}_k + \bar{B}\Delta u_k \\ y_k &= \bar{C}\bar{x}_k. \end{aligned} \tag{4}$$

Where the $\bar{A}(\gamma_k), \bar{B}$ matrices are described by (2), (3), and $\bar{A}(\gamma_k)$ is computed as a convex combination of the $\bar{A}_i$ matrices.

$$\bar{A}(\gamma_k) = \sum_{i=1}^{n_v} \lambda_i \bar{A}_i(\gamma_i), \text{with} \sum_{i=1}^{n_v} \lambda_i = 1,\ \lambda_i \geq 0, n_v = 2 \tag{5}$$

2.2 *Constrained Linear Parameter-Varying controller design*

This section presents the control design for the LCA system based on ellipsoidal invariant sets, where the uncertainty produced by the variation on the longitudinal speed is considered explicitly as a varying parameter γ_k on the formulation. In the following, the computation of an ellipsoidal contractive invariant set with a linear controller based on a parameter-dependent stabilizing gain $\Delta u_k = K(\gamma_k)\bar{x}_k$ for the constrained system is presented. This LPV controller will ensure asymptotic stability for all the states inside the domain of attraction of the controller for all the range of speed and in the absence of additive disturbances. Furthermore, in the presence of (bounded) additive disturbances, it will ensure that the states remain in a neighborhood of the origin.

The use of Linear Matrix Inequalities (LMIs) for controller design is of global nature (Boyd et al., 1994). For the sake of completeness, we recall here the description of the design of the LPV controller based on the LPV representation of the system within the polytopic uncertainty (Kothare et al., 1996). Additional constraints are added to ensure that the input and states do not saturate inside the computed ellipsoid, $\mathcal{E}(P_1) = \{x \in \mathbb{R}^n : x^T P_1^{-1} x \leq 1\}$, and the maximization in certain directions in order to enlarge the controller's domain of attraction in the states that are of higher interest.

The controller design builds up from the guaranteed decrease of the Lyapunov function, i.e.

$$\bar{x}_k^T P_1^{-1}\bar{x}_k - \bar{x}_{k+1}^T P_1^{-1}\bar{x}_{k+1} \geq \alpha \bar{x}_k^T P_1^{-1}\bar{x}_k. \tag{6}$$

where $\alpha \geq 0$. In this way, performance is ensured in terms of exponential decay of the Lyapunov function by the right hand side in (6). Now, substituting the system dynamics and considering all the vertices $i = 1...n_v$,

$$(1-\alpha)P_1^{-1} - (\bar{A}_i + \bar{B}K_i)^T P_1^{-1}(\bar{A}_i + \bar{B}K_i) > 0. \tag{7}$$

By using the Schur complement, and after pre- and post-multiplication with the symetric and full rank matrix, $blkdiag(P_1)$ we obtain the condition for $\mathcal{E}(P_1)$ to be contractive.

$$\begin{bmatrix} (1-\alpha)P_1 & P_1(\bar{A}_i + BK_i)^T \\ (\bar{A}_i + BK_i)P_1 & P_1 \end{bmatrix} \succeq 0. \tag{8}$$

The set of state constraints $\bar{X} = \{\bar{x} \in \mathbb{R}^n : H_x\bar{x} \leq b_x\}$ is symmetric and approximated by an ellipsoid for all states $i = 1...n$, $(H_{ix}/b_{ix})\bar{x} \leq 1 \Leftrightarrow F_{ix} \leq 1$. This kind of constraints can be captured by the following LMI for each state

$$\begin{bmatrix} 1 & F_{ix}P_1 \\ P_1F_{ix}^T & P_1 \end{bmatrix} \succeq 0. \tag{9}$$

In the case of input constraints, we define symmetric constraints again, $-\Delta u_{lb} = \Delta u_{ub} = \Delta u_b$. Then, we have one input constraint of the form $-\Delta u_{ib} \leq K_i\bar{x} \leq \Delta u_{ib}$, in LMI form:

$$\begin{bmatrix} \Delta u_{max}^2 & K_iP_1 \\ P_1K_i^T & P_1 \end{bmatrix} \succeq 0. \tag{10}$$

After this step, we perform a linearizing change of variables, by defining $Y_i = K_iP_1$. On top of this formulation, it may be of interest to impose the inclusion of certain reference directions defined by z_i inside the computed ellipsoid. This allows to increase the domain of attraction of the designed controller in certain directions. This means that the largest invariant ellipsoid will include the point θz_i, where θ is a scaling factor on the point direction. This kind of requirement is translated into an ellipsoidal containment constraint, $\theta z_i^T P_1^{-1}\theta z_i < 1$, that can be converted into a LMI form using the Schur complement:

$$\begin{bmatrix} 1 & \theta z_i^T \\ \theta z_i & P_1 \end{bmatrix} \succeq 0. \tag{11}$$

In the current studied application, the states x_2 and x_4 are of special interest, and inclusion constraints have been added for these directions. Finally, the last parameter that needs to be tuned is the contraction factor of the system, $(1-\alpha)$. This parameter increases the speed of convergence of the closed-loop dynamics, while decreasing the size of the obtained ellipsoid.

The objective of this controller design is to have the largest possible domain of attraction, that is, the largest positive ellipsoid that fulfills the defined invariance properties and constraints. An ellipsoid's volume is directly related to the maximization of its determinant $max\ det(P_1)$. This problem is translated into a concave problem by the use of the logarithm function $max\ logdet(P_1)$ and afterwards into a convex problem by using a minimization objective. Hence, the following LMI problem will be used to compute the maximum volume invariant ellipsoid that is maximized on directions of interest, defined by the reference directions θz_i. The problem formulation is summarized as follows

$$\min_{P_1, Y_i, \theta} \{-\theta - \sigma \text{logdet}(P_1)\} \tag{12}$$

subject to
- Invariance condition (8)
- Constraints satisfaction (9), (10).
- Point inclusion (11)

Here σ is a weighting factor included in the optimization to obtain an ellipsoid whose shape will be a trade-off between the enhanced directions and the classical maximum volume objective. Once this problem is solved (Herceg et al., 2013), (Lofberg, 2004), we obtain a common contractive invariant ellipsoid $\mathcal{E}(P_1)$ and a linear parameter-varying stabilizing gain $K(\gamma)$, providing in this way a parameter-dependent control law

$$\Delta u_k = \sum_{i=1}^{n_v} \lambda_i K_i(\gamma_k)\bar{x}_k, \text{with} \sum_{i=1}^{n_v} \lambda_i = 1,\ \lambda_i \geq 0 \tag{13}$$

2.3 *Constrained Model Predictive control design*

Model Predictive Control (MPC) design can be used to enhance the constraints handling using a finite horizon optimization, all by relaxing the linear structure of the feedback (13). In the following, a MPC strategy (Rawlings and Mayne, 2008) is studied. At each iteration, a finite-time Optimal Control Problem (OCP) is solved (14), which in turn is translated into a constrained Quadratic Programming (cQP) whose objective function is formulated from the minimization of the cost function (14) in order to obtain the optimal control input rate along the prediction horizon, subject to linear inequality constraints.

$$\begin{aligned} \min_{\Delta U}\ & J(\bar{x}_k, w_k, \Delta U) = \|\bar{x}_N\|_P^2 + \sum_{k=1}^{N-1} \|\bar{x}_k\|_Q^2 + \|\Delta u_k\|_R^2 \\ \text{s.t.}\ & \bar{x}_{k+1} = \bar{A}(\gamma_k)\bar{x}_k + \bar{B}\Delta u_k \\ & y_k = \bar{C}\bar{x}_k \\ & \bar{x} \in \bar{X},\ \Delta u \in \Delta U \\ & \bar{x}_N \in X_N \end{aligned} \tag{14}$$

with $Q \succeq 0$ and $R \succeq 0$ being the positive definite state and input weighting matrices along the prediction horizon and $\Delta U = [\Delta u_k^T, \Delta u_{k+1}^T, \ldots, \Delta u_{k+N-1}^T]^T$, $\bar{x}_k^T = [x_k^T u_{k-1}^T]^T$. In addition to this, note that only the last measured speed is known, so the system matrices will be updated each sample time and considered constant along the prediction horizon.

Finally, in order to formulate this finite-time OCP, a quadratic terminal cost P and terminal set X_N are considered to ensure system's recursive stability. In this approach, the terminal set X_N is commonly defined by the Maximal Output Admissible Set (Gilbert and Tan, 1991) adapted for the unconstrained LPV closed loop system dynamics, together with a terminal cost based on the construction of a parameter-varying Lyapunov function (Wada et al., 2004).

3. ANALYSIS OF THE ADDITIVE DISTURBANCES

Once we have defined the system dynamics, it is necessary to take into account that a vehicle encounters several elements that modify its behavior with respect to the modeled one.

This section presents the details of the sources of disturbances and then goes through the basic robust positive invariance theory and refinement tools towards a polytopic formulation, before ending up with the practical results for the LCA system.

The LPV designed in Section 2.2 exhibits a good convergence characteristics in the presence of the parameter variation, but the presence of unmodeled additive disturbances that have not been considered on the design may drive the system state out of its domain of attraction, where the controller performance is lost or, at least, not guaranteed in the presence of both constraints and parameter variation. The analysis of this aspect will be the main objective of the current section.

3.1 *System disturbances*

Perturbations can originate from several sources, such as a lateral slope on the road, difference of pressure in the tyres, actuation perturbations or crosswind. In addition to these, an important disturbance is the curvature of the road w_k, due to its direct influence on the steering input signal. This perturbation affects the lateral dynamics behavior of the system, by adding an extra term to the lateral equations of motion, which is related to the centripetal acceleration $-v_x^2\rho$ that appears when driving in a curve. Furthermore, the resulting steering angle needs to be the addition of the input signal needed to steer the vehicle to the center of the road and the angle needed to follow the curve. In this way, the closed-loop system dynamic equations (4) are extended in order to contain the curvature of the road effects, modeled by a bounded additive disturbance $w_k \in \mathcal{W}$

$$\bar{x}_{k+1} = \left(\bar{A}(\gamma_k) + \bar{B}K(\gamma_k)\right)\bar{x}_k + \bar{E}(v, v^2)w_k, \tag{15}$$

with $(\bar{A}(\gamma_k) + \bar{B}K(\gamma_k))$ being the closed-loop form of the system dynamics and denoted by $\bar{A}_C(\gamma_k)$ in the following. The closed loop system will ensure the nominal stability based on the certificates offered by the parameter-depending Lyapunov function. Moreover, $\bar{E} = \left[0, -v, -v^2, 0, 0\right]^T \in \mathbb{R}^{n\times p}$, thus we have a parameter-varying disturbances matrix. In the following, three modeling abstractions are presented in decreasing conservativeness order.

Superposition principle To begin with, the two realizations of the speed parameter, v and v^2 are defined respectively as ν_1 and ν_2, yielding $\bar{E}(\nu_{1_k}, \nu_{2_k})$. Due to the linearity of the dynamics of the parameter-varying matrix $\bar{E}(\nu_1, \nu_2)$, a superposition principle can be employed in order to separate the influence of the two uncertainty sources, $\bar{E}(\nu_1, \nu_2) = \bar{E}_1(\nu_1)+\bar{E}_2(\nu_2)$, and analyze independently their impact on the closed loop dynamics. Again, this parameter uncertainty can be embedded in a polytopic approach, obtaining each value inside the bounded working range of speed as a convex combination of the two extreme values:

$$E(\nu_{1_k}, \nu_{2_k}) = \sum_{i=1}^{n_v} \beta_i E_{1_i}(\nu_{1_k}) + \sum_{i=1}^{n_v} \eta_i E_{2_i}(\nu_{2_k}), \tag{16}$$

with $\sum_{i=1}^{n_v} \beta_i = 1,\ \beta_i \geq 0, \sum_{i=1}^{n_v} \eta_i = 1,\ \eta_i \geq 0$ and the matrix $\bar{E}$ defined by the addition of the matrices $\bar{E}_1$ and $\bar{E}_2$, that are linear on the corresponding parameters, $\bar{E}(\nu_{1_k}, \nu_{2_k}) = \bar{E}_1(\nu_{1_k}) + \bar{E}_2(\nu_{2_k}) = [0, -\nu_{1_k}, 0, 0, 0]^T + [0, 0, -\nu_{2_k}, 0, 0]^T$.

Moreover, the dependency of the matrices $\bar{E}_1$ and $\bar{E}_2$ on the parameters ν_{1_k}, ν_{2_k} can be eliminated by scaling the disturbances boundaries with the maximum values of the parameter:

$$\begin{aligned}\bar{x}_{k+1} &= \bar{A}_C(\gamma_k)\bar{x}_k + \bar{E}(\nu_{1_k}, \nu_{2_k})w_k = \\ &= \bar{A}_C(\gamma_k)\bar{x}_k + \bar{E}_1(\nu_{1_k})w_k + \bar{E}_2(\nu_{2_k})w_k = \\ &= \bar{A}_C(\gamma_k)\bar{x}_k + \bar{E}_1 \underbrace{\nu_1 w_k}_{w_{1_k}} + \bar{E}_2 \underbrace{\nu_2 w_k}_{w_{2_k}},\end{aligned} \tag{17}$$

where $\bar{E}_1 = [0, -1, 0, 0, 0]^T$ and $\bar{E}_2 = [0, 0, -1, 0, 0]^T$ are now parameter independent constant matrices, and the pair of redefined disturbances are $w_{1_k} \in \mathcal{W}_1$, $w_{2_k} \in \mathcal{W}_2$, with $\mathcal{W}_1 = \nu_{1_{max}}\mathcal{W}$ and $\mathcal{W}_2 = \nu_{2_{max}}\mathcal{W}$.

Note however, that the superposition of the effects will only offer a over approximation as long as the co-variance of the sources of disturbances is lost. This feature can be treated when a refinement of an initial robust positive invariant will be performed in view of the characterization of the minimal robust positive invariant set (Section 3.3).

Worst case polytopic representation In order to preserve the existing relationship in between the parameters ν_1 and ν_2 it can be taken into account that the domain of variation of ν_1, ν_2 is certainly defined by the curve $f(v) = v^2$, scaled by the constant value ρ_m, which is the maximal value of the road curvature. This curve can be represented by a polytopic embedding, approximated for example by a trapezoidal shape (Fig.2) for the sake of simplicity of the vertex representation. This is first limited by the segment $[\rho_m\nu_{1_{min}}, \rho_m\nu_{2_{min}}], [\rho_m\nu_{1_{max}}, \rho_m\nu_{2_{max}}]$. Then, we consider a line which is parallel to the first segment and tangent to the curve and the last two edges are defined by intersection of this line and the ones tangent at the extreme vertex. This provides a polyhedron with four vertices, $n_v = 4$, each one defining a $\bar{E}_i$ such that $E(\nu_{1_k}, \nu_{2_k}) = \sum_{i=1}^{n_v} \alpha_i \bar{E}_i(\nu_{1_k}, \nu_{2_k})$ with $\sum_{i=1}^{n_v} \alpha_i = 1$ and $\alpha_i \geq 0$. Alternatively, a containment optimization problem can be performed (Lombardi et al., 2009) to obtain a tight polyhedral embedding of the curve on Fig. 2. Still, it is necessary to note that we are considering the same

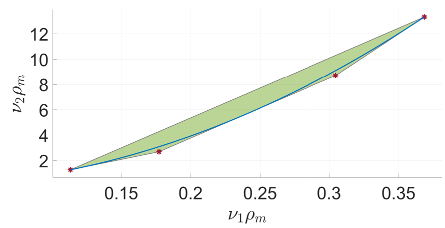

Fig. 2. Polytopic approximation of the curve $v\rho_m = v^2\rho_m$

maximal value of the curvature of the road ρ_m for all the range of speed, which remains an important source of conservativism, as road conception directives (Vertet and Giausserand, 2006) dictate from the early design stage of the infrastructure facilities that the road curvature and the set speed are directly related. These elements are considered in the next formulation and integrated in the additive disturbance analysis.

Refined polytopic representation Following up with the previous formulation, it is possible to go forward by means of considering that the maximal value of the curvature is speed-dependent too, that is, there exists a series of rules and conventions that are taken into account when the roads are designed, in order to ensure safety and comfort of the citizens. These conventions set a tight relation between the speed limit at a given road and the minimal radius for the road profile. When

Table 1. Radius-speed values for design on highways (Vertet and Giausserand, 2006)

	50kmh	70kmh	90kmh	110kmh	130kmh
Comfort R_{min}(m)	98	242	473	808	1267
Safety R_{min}(m)	66	162	318	541	848

we consider this formulation, we are indeed reducing the conservatism of the previous two formulations (Fig. 3).

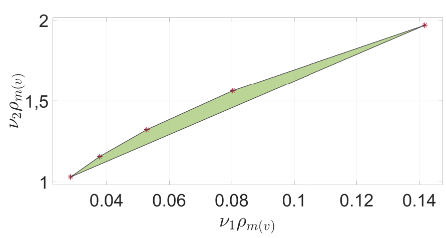

Fig. 3. Polyopic representation from Table 1 data (comfort)

3.2 Robust invariance condition

Consider the LPV closed loop dynamics (15), with $w_{j_k} \in \mathcal{W}_j = \{w_j^T w_j \leq 1\}$. The starting point will be the fact that an ellipsoid $\mathcal{E}_P = \{\bar{x}P^{-1}\bar{x} \leq 1\}$ is robust positive invariant if $\forall \bar{x} \in \mathcal{E}_P$ then $\bar{A}_C(\gamma)\bar{x} + \bar{E}_j w_j \in \mathcal{E}_P, \forall w_j \in \mathcal{W}_j$ and $\forall v \in \mathcal{V}$. In other words, starting from any point in $\mathcal{E}_P$, the state of the system will not leave the set under any admissible parameter variation and disturbance.

Theorem 3.1. The ellipsoid $\mathcal{E}_P$ is invariant for system (15) if and only if there exists a positive definite matrix $P \in \mathbb{R}^{nxn}$

$$\begin{bmatrix} (1-\tau)P & \mathbf{0} & P\bar{A}_{i_C}^T \\ \mathbf{0} & \tau I & \bar{E}_j^T \\ \bar{A}_{i_C}P & \bar{E}_j & P \end{bmatrix} \succeq 0, \tag{18}$$

for all $i = 1 \ldots n_v$ $0 < \tau < 1$. ■

Readers are referred to (Nguyen et al., 2015), (Luca et al., 2011) for proof of Theorem 3.1.

3.3 Refinement of the Robust Positive Invariant set

The polyhedral representation of the RPI sets give a better approximation of the domain of attraction, but they have a major issue: complexity is not fixed by the dimension of the state-space, and they can become highly complex very fast.

In order to refine the obtained ellipsoid by means of the formulation introduced in this section and obtain an approximation of the RPI set, a recursive strategy is used (Olaru et al., 2010). For this final refinement of the RPI set, we approximate the initial ellipsoidal set $\mathcal{E}_{P_0}$ by a s-vertices polyhedron Ω_0. After this, we compute the forward sequence as shown in Algorithm 1 in order to obtain the RPI polyhedral approximation.

Remark 1. When using the decoupled strategy for the additive disturbances (Subsection 3.1.1), the refined RPI will be obtained by applying Algorithm 1 to an initial polyhedral set Ω_0 defined by the convex hull of the obtained RPI set for each disturbance, w_1 and w_2.

$$\Omega_0 = \text{ConvHull}_{j=1}^{n_w}\Omega_{j_0} \tag{19}$$

Algorithm 1: RPI set refinement

Data: Polyhedral approximation Ω_0 of computed RPI $\mathcal{E}_{P_0}$
Result:
1) Compute the image set for each one of the LPV system dynamic realizations using the A_{i_C} transformation. The set that keeps the invariance property is the convex hull of the resulting sets and addition by Minkowski sum of the worst case additive disturbances.

$$\Omega_{k+1} = \text{ConvHull}\{A_{i_C}\Omega_k\} \oplus \text{ConvHull}\{E_i\mathcal{W}\} \tag{20}$$

2) Repeat 1) until $\Omega_{k+1} = \Omega_k$ or up to N_{max} iterations.
Return Refined RPI set

3.4 RPI results and analysis

In the following, the tools shown in the previous section to construct the RPI set (18) are used to offer a certification on the behavior of the LPV controller (13) in a curved road. It is worth noticing that an alternative technique that can be used to compute the RPI sets is presented in (Martínez, 2015) based on the Bounded Real Lemma argument in the present work we use the Theorem 3 from this analysis.

Remark 2. A set Ω_∞ is called minimal Robust Positively Invariant (mRPI) set if it is a RPI set in $\mathbb{R}^n$ contained in every RPI set.

The size of this set provides a measurement of the uncertainty that the bounded disturbances produce on the closed loop dynamics of a system: the larger the mRPI set is, the more the system is affected by the disturbances. Given the closed loop dynamics of our system $A_C(\gamma_k)$ with a linear parameter-varying stabilizing gain $K(\gamma_k)$, the BMI problem (18) is solved for different τ values with a criterium based on the minimization of the trace(P^{-1}), obtaining a family of RPI. The value for the positive scalar τ is set so that (18) yields the smaller RPI ellipsoid, denoted by $\mathcal{E}(P_2)$. The final objective here is to provide a certificate that the designed controller would keep its performance in the presence of the bounded additive disturbances. In order to do so, we can check the containment of the mRPI set inside the domain of attraction of the controller: if $\mathcal{E}(P_2) \subseteq \mathcal{E}(P_1)$, the controller performance is maintained in a set $\Omega = \mathcal{E}(P_1) \ominus \mathcal{E}(P_2)$, that can be approximated by the ellipsoid $\mathcal{E}(P'_N)$. This is refined (Algorithm 1) in order to obtain a suitable terminal set X_N for the MPC strategy (Section 2.3).

Along these lines, the corresponding mRPI set has been computed for the closed-loop auto-steering system, and proves to not be included in the domain of attraction of the nominal LPV control. This is not surprising since the tuning of the LPV controller is done based on aggressive contractiveness objectives in spite of robustness. This means that the performance of this controller is not kept for any speed-curvature variation. In practice, what can be done is the computation of the maximal range of speed variation that would be admissible for a given curvature value, naming *admissible* those speed limit values that provide a mRPI set which is smaller than $\mathcal{E}(P_1)$. In Fig.(4), the speed ranges for which the computed $\mathcal{E}(P_2) \subseteq \mathcal{E}(P_1)$ for fixed curvature values are shown [1] . It can be seen that for lower

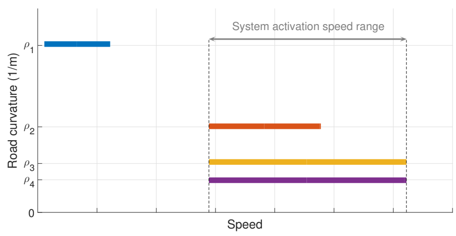

Fig. 4. Admissible speed range in curve for the parameter-varying controller (Section 2.2) for fixed ρ values

curvature values the controller could be suitable in part of the speed range activation zone. However, if the curvature is higher, this kind of control would not be able to control the lateral dynamics of the system unless the speed was much lower than the range activation of the LCA system. Moreover, the size of the computed mRPI sets is relatively big compared to the size of the controller domain of attraction $\mathcal{E}(P_1)$ (Fig. 5), so the resulting invariant set X_N obtained from the refinement of $\mathcal{E}(P'_N)$ turns out to be relatively small.

[1] Due to confidentiality reasons the numerical details on the speed range and curvature values are omitted from the figure

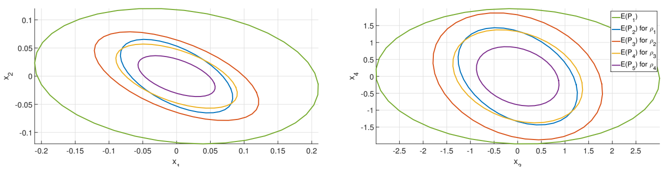

(a) $\text{Proy}(x_1, x_2)$ plane (b) $\text{Proy}(x_3, x_4)$ plane

Fig. 5. Computed mRPI set $\mathcal{E}(P_i)$ for fixed ρ_i values (Fig. 4)

4. CONTROL REDESIGN FOR BUILT-IN ROBUSTNESS WITH RESPECT TO ADDITIVE DISTURBANCES

The results of the robustness analysis of the designed LPV stabilizing controller provided by the RPI theory tools (Section 3) show that such strategy would not be a proper option when driving in a curved road, unless the driving conditions were fixed and limited in terms of speed-curvature values. This assumption needs to be revisited if the driving situations need to cover a large range of speed-curvature. Regarding this, we proceed to the reformulation of the proposed controllers, obtaining a robust control strategy from the design stage. This will impact the terminal cost and terminal set, that will be provided by the maximal RPI set computed in the presence of parameter variations and bounded additive disturbances.

4.1 LPV controller redesign

The MPC terminal cost and terminal set will be based on the construction of a parameter-dependent Lyapunov function and the associated RPI set. For this construction, in spite of pre-computing a stabilizing gain for the unperturbed system, the stabilizing gain computation is done at the same time as the RPI set computation, obtaining in this way a robust stabilizing gain that maximizes the RPI set, in which the input and output constraints are fulfilled in the presence of parameter-varying disturbances. This can be done by solving the following LMI problem (Nguyen et al., 2015)

$$\max_{P_3, Y_i, \theta} \{\theta + \sigma \text{trace}(P_3)\} \tag{21}$$

subject to: • Invariance contidion

$$\begin{bmatrix} (1-\tau)P_3 & \mathbf{0} & P_3\bar{A}_i^T + Y_i^T\bar{B}^T \\ \mathbf{0} & \tau I & \bar{E}_j^T \\ \bar{A}_iP_3 + \bar{B}Y_i & \bar{E}_j & P_3 \end{bmatrix} \succeq 0, \tag{22}$$

for all $i = 1 \ldots n_v$, $j = 1 \ldots n_v$ and $K_{3_i} = Y_i P_3^{-1}$.

- Constraints satisfaction (9), (10).
- Point inclusion (11)

The obtained parameter-varying linear state feedback gain provides a parameter-dependent control law with $\Delta u_k = \sum_{i=1}^{n_v} \lambda_i K_{3_i}(\gamma_k)\bar{x}_k$ with $\sum_{i=1}^{n_v} \lambda_i = 1$, $\lambda_i \geq 0$ which maximizes the size of the RPI set in the presence of system constraints and disturbances with the final goal of ensuring robust stability for the MPC strategy presented in the following, where the terminal set is defined as the polyhedral refinement of $\mathcal{E}(P_3)$, $\tilde{X}_N = \Omega(\mathcal{E}(P_3))$.

4.2 Curvature of the road: exploit local information on the disturbances realization

Up to this point the curvature has been considered in terms of its bounded variation without any supplementary restrictions. However, local information on the longitudinal direction can be used for extrapolation. This will transform the MPC prediction model to include the curvature of the road.

Within this framework, it is necessary to foresee the geometry of the road trajectory. In this paper, a third order polynomial is used $c(\chi) = c_0 + c_1\chi + c_2\chi^2 + c_3\chi^3$, where χ represents the longitudinal distance with respect to the current position of the vehicle and c_i are the online measured coefficients of the reference trajectory that approximates the lane. From this model, it is possible to compute the curvature of the road at any distance χ_k where we will be at any future time k by means of equation (23), where $(.)'$ implies the derivative of the polynomial with respect to χ.

$$w_k = \frac{c''(\chi_k)}{(1 + c'(\chi_k))^{(3/2)}} \tag{23}$$

4.3 MPC redesign

When there is a prediction model available (23) to calculate the incoming additive disturbance along the prediction horizon N, the effect of the additive disturbance can be incorporated to the predictive control strategy (J.M.Maciejowski, 2002) by including their effect on the system dynamics model (15) and approximately cancel it by a suitable control action, commonly known as *feedforward* control. The final MPC problem formulation is stated in the following

$$\begin{aligned} \min_{\Delta U} \; & J(\bar{x}_k, w_k, \Delta U) = \|\bar{x}_N\|_{P_3}^2 + \sum_{k=1}^{N-1} \|\bar{x}_k\|_Q^2 + \|\Delta u_k\|_R^2 \\ \text{s.t.} \; & \bar{x}_{k+1} = \bar{A}(\gamma_k)\bar{x}_k + \bar{B}\Delta u_k + \bar{E}(\nu_{1_k}, \nu_{2_k})w_k \\ & y_k = \bar{C}\bar{x}_k \\ & \bar{x} \in \bar{X}, \; \Delta u \in \Delta U \\ & \bar{x}_N \in \tilde{X}_N \end{aligned} \tag{24}$$

with Q, R, ΔU and $\bar{x}_k$ defined as in Section 2.3 and w_k being the curvature of the road. Finally, the quadratic terminal cost P_3 and terminal set $\tilde{X}_N$ are defined by the maximal RPI obtained when solving (21).

4.4 Simulation

Performance of the designed MPC when driving on a curved road with varying speed is shown via a numerical simulation.

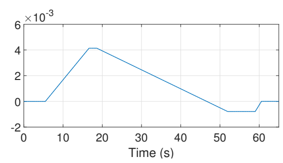

Fig. 6. MPC simulation: curve profile $[1/m]$

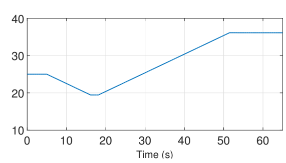

Fig. 7. MPC simulation: speed profile $[m/s]$

In Fig. 9, the time evolution of the lateral offset of the vehicle together with the expected offset produced by the disturbances (measured via mRPI analysis) are shown. It can be seen that the simulation is started from a perturbed state. In the first phase, the control input (Fig. 10) variation reaches its limit, in order to drive the vehicle to the center of the road. Then, the road enters in the curve phase, together with variations on the speed vehicle, inducing an error on the lateral position, which again

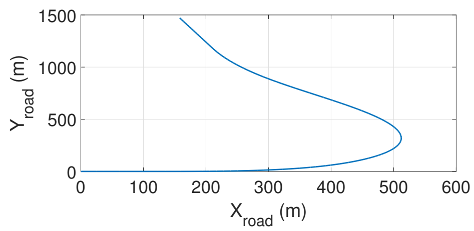

Fig. 8. MPC simulation: road profile

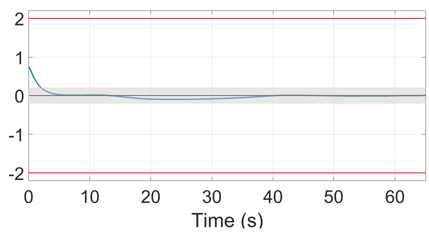

Fig. 9. MPC simulation: Lateral offset $y_{CoG}[m]$

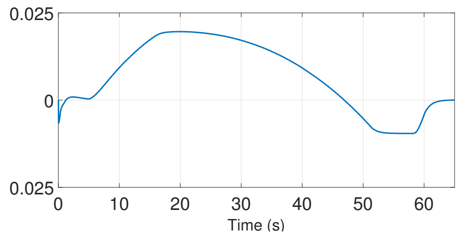

Fig. 10. MPC simulation: Steering angle δ_c

will be progressively corrected by the steering angle. It can be seen that the controller shows a satisfactory performance and it is able to stabilize the dynamics of the system in the presence of the variation of speed, curvature and the white noises.

5. CONCLUSION

LCA system dynamics modeling in the presence of speed variation have been described by a parameter-varying model, where the parameter is bounded and measured. In the same way, different methods for modeling the effects of a curved road on the system have been introduced, by means of different parameter-varying additive disturbances models which differ on the level of conservativeness.

In addition to this, robust positive invariance theory has been exploited as a main tool to certify the behavior of a LPV controller that does not take the impact of the additive disturbances into account on the design stage. Nevertheless, its working area is highly limited, and a Model Predictive Control strategy that predicts the curvature of the road by means of a polynomial model and anticipates to its effect is considered. Moreover, a terminal cost and a parameter-varying stabilizing gain that maximizes the robust terminal set in the presence of system constraints and the modeled additive disturbances are designed to ensure the controller recursive stability for such scenarios.

From the application point of view, the system studied in the present work has been simplified to provide a scenario where the attention is focused on the impact of the additive disturbances. There are more features which could be included in future controllers. These include actuator dynamics and the consideration of parameter-varying input constraints.

REFERENCES

Bemporad, A. and Morari, M. (1999). Robust model predictive control: A survey. In *Robustness in identification and control*, 207–226. Springer.

Bokor, J. and Balas, G. (2005). Linear parameter varying systems: A geometric theory and applications. In *16th IFAC World Congress, Prague*, volume 1, 1–11.

Boyd, S.P., El Ghaoui, L., Feron, E., and Balakrishnan, V. (1994). *Linear matrix inequalities in system and control theory*, volume 15. SIAM.

Gilbert, E.G. and Tan, K.T. (1991). Linear systems with state and control constraints: The theory and application of maximal output admissible sets. *Automatic Control, IEEE Transactions on*, 36(9), 1008–1020.

Herceg, M., Kvasnica, M., Jones, C.N., and Morari, M. (2013). Multi-parametric toolbox 3.0. In *Control Conference (ECC), 2013 European*, 502–510. IEEE.

J.M.Maciejowski (2002). *Predictive control with constraints*. Prentice Hall.

Kothare, M.V., Balakrishnan, V., and Morari, M. (1996). Robust constrained model predictive control using linear matrix inequalities. *Automatica*, 32(10), 1361–1379.

Lofberg, J. (2004). Yalmip: A toolbox for modeling and optimization in matlab. In *Computer Aided Control Systems Design, 2004 IEEE International Symposium on*, 284–289.

Lombardi, W., Olaru, S., and Niculescu, S.I. (2009). Invariant sets for a class of linear systems with variable time-delay. In *Control Conference (ECC), 2009 European*, 4757–4762.

Luca, A., Rodriguez-Ayerbe, P., and Dumur, D. (2011). Invariant sets techniques for Youla–Kučera parameter synthesis. *International Journal of Control*, 84(9), 1553–1564.

Martínez, J.J. (2015). Minimal RPI sets computation for polytopic systems using the bounded-real lemma and a new shrinking procedure. *IFAC-PapersOnLine*, 48(26), 182–187.

Nguyen, H.N., Olaru, S., Gutman, P.O., and Hovd, M. (2015). Constrained control of uncertain, time-varying linear discrete-time systems subject to bounded disturbances. *IEEE Transactions on Automatic Control*, 60(3), 831–836.

Ni, L., Gupta, A., Falcone, P., and Johannesson, L. (2016). Vehicle lateral motion control with performance and safety guarantees. *IFAC-PapersOnLine*, 49(11), 285–290.

Olaru, S., De Doná, J., Seron, M., and Stoican, F. (2010). Positive invariant sets for fault tolerant multisensor control schemes. *International Journal of Control*, 83(12), 2622–2640.

Pacejka, H. (2005). *Tire and vehicle dynamics*. Elsevier.

Pannocchia, G. and Rawlings, J.B. (2001). The velocity algorithm LQR: a survey.

Rajamani, R. (2006). *Vehicle dynamics and control*. Springer.

Rawlings, J.B. and Mayne, D. (2008). Model predictive control. In *The 2008 Spring National Meeting*.

Sename, O., Gaspar, P., and Bokor, J. (2013). *Robust control and linear parameter varying approaches: application to vehicle dynamics*, volume 437. Springer.

Vertet, M. and Giausserand, S. (2006). *Comprendre les principaux paramètres de conception géométrique des routes*. Sétra.

Wada, N., Saito, K., and Saeki, M. (2004). Model predictive control for linear parameter varying systems using parameter dependent Lyapunov function. In *Circuits and Systems, 2004. MWSCAS'04. The 2004 47th Midwest Symposium on*, volume 3, iii–133. IEEE.